ARTICLE
JOURNAL OF UNIVERSITY OF BABYLON
For ENGINEERING SCIENCES (JUBES)
Vol.31, No.6.| 2023

Intelligent Control of Switched Reluctance Motor for Electrical Vehicle Applications with Different Controller

Ahmed Fawzi Jasim[1], Fadhel A. Jumaa[2],.Ali A. Abdullah Albakry[3]
[1,2] Department of Electrical Power Engineering Techniques, Al-Mussaib Technical College Al-Furat Al-Awsat Technical University Babil, Iraq.
[3)] Al Mamoun University College, Electrical Power Engineering, Iraq.
ahmed.fawzi.tcm.22@student.atu.edu.iq
dr-fadhela.jumaa@atu.edu.iq
Ali.a.albakry@almamonuc.edu.iq.

Received:	20/6/2023	Accepted:	23/8/2023	Published:	20/9/2023

Abstract

Switched reluctance motors (SRM) are used to produce a lot of torque when they are operating at high magnetic saturation. Due to the high magnetic saturation, the relationship between phase current, rotor position, and the flux linkage of SRM is nonlinear. Noise, disturbances, and inertia of load torque can all have a negative impact on the SRM driver system's speed controller performance. In this study, the SRM driver system's sliding mode controller was developed .The sliding mode controller(SMC) speed controller was used to regulate speeds of the SRM throughout a wide range speeds, including high and low speeds. This study compares (SMC) with a modified reaching law and a Proportional Integral Divertive Control (PID) controller for a 6/4 pole SRM using an optimization technique for switching controllers. Furthermore, the rotor speed was simulated and compared to the reference speed. The Exponential Sliding Mode Controller (ExpSMC) is the best in terms of performance and robustness for an electric vehicle application, depending on a simulation of an established test bench using the two controllers.

Keywords: Exponential Sliding mode controller, Proportional Integral Divertive PID, switched reluctance motor, Electric vehicle.

1.Introduction

In recent years, industries have given more thought to induction motors (IM), permanent magnet synchronous motors (PMSM), and switching reluctance motors (SRM). SRM stands out among these motors thanks to its straightforward and robust design [1-4]. Also, the SRM's rotor contains neither magnets nor windings; instead, the stator poles have just windings. Furthermore, low-cost silicon, sheets with a doubly. salient structure are used to make the stator and rotor. SRM is strong and able to operate in extreme temperatures and demanding operational situations. Because their fault tolerance, low inertia, low maintenance requirements, high efficiency, high torque--generating capacity, simple speed control, SRMs are used in a variety of industrial. applications, including servomotor drives, home appliances, electric aircraft wind turbines, electric vehicles, and air conditioning fans [5-9].

ISSN: 2616 - 9916
www.journalofbabylon.com | Journal.eng@uobabylon.edu.iq | info@journalofbabylon.com

ISSN: 2616 - 9916
www.journalofbabylon.com | Journal.eng@uobabylon.edu.iq | info@journalofbabylon.com

However, the SRM's electromagnetic torque ripple is brought on by the stator and rotor poles' double salient construction [10]. Due to radial forces, the motor also exhibits acoustic noise and vibration problems [11]. Also, it can be hard to model SRM and high-performance speed control in a dynamic way because the torque generation and inductance change in a way that is not linear and depends on phase current and rotor position[12]. Back electromotive force (EMF) makes it hard to control SRM drivers, but recent improvements in power electronics, digital signal processors, and sensors have made it possible to run SRM drivers at a wide range of speeds. This lead to the creation of a number of ways to control the current, such as ramp comparison control with constant switching frequency, hysteresis control, and adaptive sliding current control. Traditional PI controllers are not advised for use with SRM drives since they are ineffective at controlling non-linear control systems [13]. proposes an integral saturation problem-free switching variable proportional desaturation PI regulator that provides better dynamic performance and speed control stability throughout all stages of operation. However, consideration must be given to dynamic performance stability at higher operating speeds, as well as torque ripple pulsations and the inherent flaws of mathematical models [14]. PID control, sliding mode control, and higher-order sliding mode control based on the slide mode control algorithm are all presented concurrently for the proposed control strategy's current and velocity loops. Even if they are long-lasting, expositional sliding mode control is still the best way to eliminate chattering, particularly in electric car applications [15]. In fact, as other applications depend on the dynamic behavior. of the vehicle where the/model of the vehicle drivetrain is taken into consideration, they can be improved with the enhancement of vehicle drivetrain performances utilizing SRM and ExpSMC control. The angle estimate in vision-aided intelligent vehicles that sideslip is based on a dynamic model[15-16].

The main contribution of this paper are focused on the following

- Performance comparison of Exponential Sliding Mode Controller (ExpSMC)and Proportional Integral Divertive Control (PID) for the current and speed control of SRM control strategy. These control are developed and validated by simulation
- The speed ripple and finite time convergence are simultaneously minimized ,and the undesired chattering effect under load and a wide speed range are reduced
- Finally ,performance compression are carried with the collected simulation data showing that the Exponential Sliding Mode Controller is the best control to select for the improvement of electrical vehicle drivetrain performance

2. Mathematical Model of SRM

By neglecting the mutual inductance among the phases, it is feasible to formulate the equivalent circuit for the SRM in the subsequent manner [16],[17],[18],[19].

The voltage applied to any phase is given by:

$$V = R_{ph} i + \frac{d\lambda(\theta,i)}{dt} \quad (1)$$

Where Rph represents the resistance per phase and λ denotes the flux linkage per phase, the flux linkage is determined by:

$$\lambda(\Theta,i)=L(\Theta,i)i \quad (2)$$

ISSN: 2616 - 9916
www.journalofbabylon.com | Journal.eng@uobabylon.edu.iq | info@journalofbabylon.com

The phase voltage equation is expressed as follows, considering that the inductance (L) is dependent on the phase current and rotor position:

$$V = R_{ph} i + L(\theta, i)\frac{di}{dt} + i\frac{d\theta}{dt}\frac{dL(\theta,i)}{d\theta} \quad (3)$$

$$V = R_{ph} i + L(\theta, i)\frac{di}{dt} + iw.\frac{dL(\theta,i)}{d\theta}) \quad (4)$$

The induced electromotive force (emf), obtained as e, is calculated as follows:

$$e = \frac{(dL(\theta,i))}{d\theta} w_m i = K_b w_m i \quad (5)$$

The emf constant, Kb, is defined as follows:

$$K_b = \frac{dL(\theta,i)}{d\theta} \quad (6)$$

The emf constant, Kb, is dictated by the system's operating point and can be derived by measuring it at a constant current at that point. Figure1 depicts the analogous circuit for the switched reluctance motor (SRM) with only one phase using the voltage expression and the equation for the induced emf.

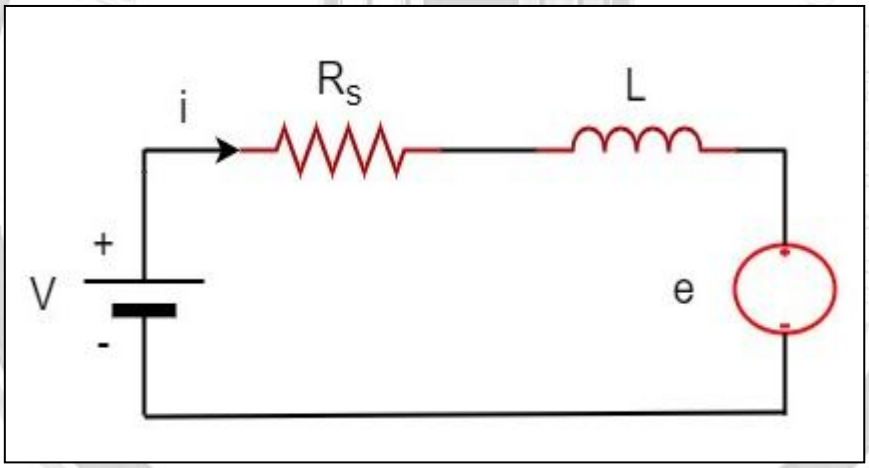

Figure 1: One-phase Equivalent Circuit of SRM

The power can be calculated as follows:

$$P = vi = R_s i^2 + i^2 \frac{dL(\theta,i)}{dt} + L(\theta, i)\, i\frac{di}{dt} \quad (7)$$

In order to draw a meaningful conclusion, the last term can be expressed in terms of known variables as follows

$$\frac{d}{dt}\left(\frac{1}{2} i^2 L(\theta, i)\right) = L(\theta, i)\frac{di}{dt} + \frac{1}{2} i^2 \frac{dL(\theta,i)}{dt} \quad (8)$$

The power equation is given by:

$$P_i = vi = R_{ph} i^2 + L(\theta, i) I \frac{di}{dt} + \frac{1}{2} i^2 \frac{dL(\theta,i)}{dt} \quad (9)$$

Pi stands for the instantaneous power supply. The input power is made up of the sum of the resistive losses, the rate of change of field energy, and the air gap power (pa), which is described as (L(, i) * i2/2). By putting time in terms of where the rotor is and how fast it is going, the equation can be written as:

$$dt = \frac{d(\theta)}{w} \quad (10)$$

The air gap power yields the following expression

$$P_a = \frac{1}{2} i^2 \frac{dL(\theta,i)}{d(\theta)} \frac{d(\theta)}{dt} \quad (11)$$

The air gap power is defined as follows:

$$P_a = w_m T_e \quad (12)$$

The electromagnetic torque is calculated using equations (11) , (12) as follows

$$T_e = \frac{1}{2} i^2 \frac{dL(\theta,i)}{d(\theta)} \quad (13)$$

3. Speed Control for Switched Reluctance Motor

The speed of the motor is sensed through a speed sensor which is converted into a signal (w_m). This signal is compared with a reference or desired signal to generate the error signal which equals the difference between the desired speed and the (w_m). The error signal is fed to a speed controller to let the actual motor speed equal to the desired speed . reduce the error value to zero. The controlling signal that is generated from the speed controller is modulated through a pulse width modulation (PWM) technique which generates the required pulses for each driver-switching device. On the other hand, to synchronize the generated pulses with the motor position, the (w_m) is integrated to get the rotational angle which is fed to the position sensor as shown in Figure 3. for the rotor position calculations. For precise synchronization, both the PWM signal and the generated signal from position sensors are logical operator (AND gate) to get the required pulses for the insolated gate bipolar transistor 6 IGBT switching devices in the motor driver.

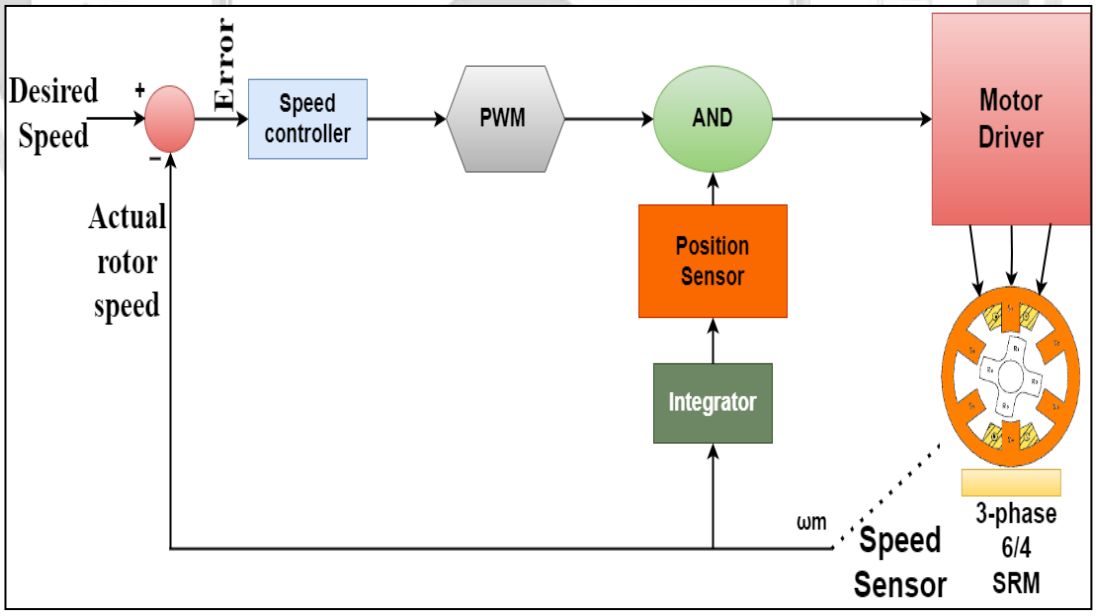

Figure 2: Block Diagram of PWM Mode of Operation

4. Speed Control Methods

In this research, the speed of an SRM is controlled through several methods like PID controller and slide mode controller.

4.1 PID Controller

For many years, the proportional integral derivative (PID) controller is considered one type of conventional controller which are employed in countless applications. It is constructed from three types of controllers named proportional (P) and Integral (I), and

ISSN: 2616 - 9916
www.journalofbabylon.com | Journal.eng@uobabylon.edu.iq | info@journalofbabylon.com

ISSN: 2616 - 9916
www.journalofbabylon.com | Journal.eng@uobabylon.edu.iq | info@journalofbabylon.com

Derivative (D) [20]When the error signal is fed to this controller, it will generate the required control signal (t) such that:

$$u(t) = e(t)\,K_P + k_I \int e(t)dt + K_D \frac{d}{dt} e(t) \qquad (14)$$

where K_P, k_I, and K_D are representing the proportional, integral, and derivative gains respectively. These gains can be tuned in several methods based on the system response. They can be tuned manually by the Ziegler-Nichols method, or automatically through using optimization techniques[21]. The implementation flow chart is shown in Figure 3

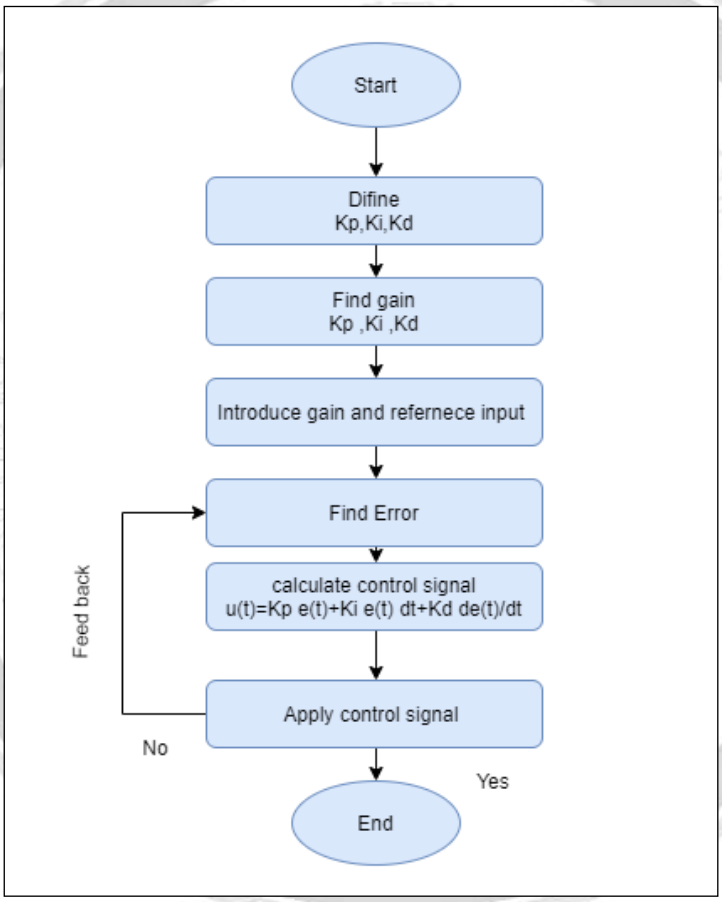

Figure 3: Flow Chart of PID Implementation

4.2. Sliding Mode Controller

It can be considered that the sliding mode controller (SMC) is one kind of nonlinear, discontinuous, and robust technique [22].It is more appropriate to regulate systems which its configuration may change during its normal operating conditions[23]. It is slides the system states on such a surface which is called as "sliding surface" as shown in Figure (4)

ISSN: 2616 - 9916
www.journalofbabylon.com | Journal.eng@uobabylon.edu.iq | info@journalofbabylon.com

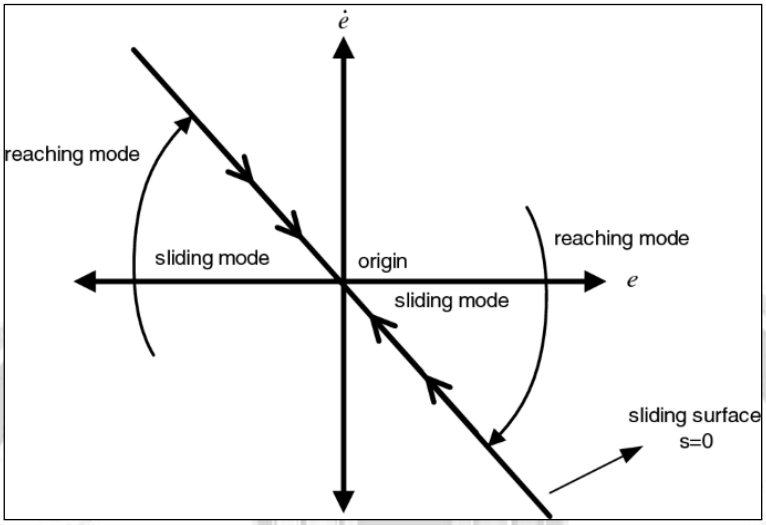

Figure 4: The Idea of Sliding Mode[24].

In general, SMC places the state variables of the controlled system near the sliding surface[24]. Let's suppose that the state variables are represented by the error e and change of error with time $\dot{e}$. Let's suppose that the error e is the difference between desired speed and the motor rotational speed. In order to make these state variables in asymptotic convergence then e and $\dot{e}$ should reach zero i.e. $\lim_{t\to\infty} e, \dot{e} = 0$ Where [25]:

$$e(t) = e(0)\, e^{-c\,t} \tag{15}$$

$$\dot{e}(t) = -\,c\, e(0)\, e^{-c\,t} \tag{16}$$

where the constant $c > 0$. In this case can introduce a new variable called "σ" where:

$$\sigma = \sigma(e, \dot{e}) = \dot{e} + c\, e \tag{17}$$

It is required to drive σ sliding variable to be zero in finite time to provide a controlling variable named as "u". This can be made through applying of "Lyapunov function techniques" to the σ dynamics where:

$$\dot{\sigma} = c\,\dot{e} + f(e, \dot{e}, t) + u\,, \qquad \sigma(0) = \sigma_0 \tag{18}$$

There are many kinds of SMC where in this chapter we talks briefly about two of them.

4.2.1 Exponential Sliding Mode Controller

In exponential SMC or (ExpSMC) it can be identified by the following mathematical expressions where [26]:

$$u = \frac{K}{N(\sigma)}\, sign(\sigma)\,, \qquad k > 0 \tag{19}$$

then

$$N(\sigma) = \delta_0 + (1 - \delta_0)\, e^{(-\alpha|\sigma|^p)} \tag{20}$$

where p is a strictly positive integer, α is also strictly positive, and δ_0 is a strictly positive offset less than 1. For each SMC, the sign function is defined by:

$$sign(\sigma) = \begin{cases} 1 \;\; if\; \sigma > 0 \\ -1\; if\; \sigma < 0 \end{cases} \tag{21}$$

ISSN: 2616 - 9916
www.journalofbabylon.com | Journal.eng@uobabylon.edu.iq | info@journalofbabylon.com

One of the drawback of SMC is the effect of chattering on the controlling signal *u(t).* In order to decrease the chattering effect, it is desirable to replace $sign$ function by hyperbolic tan $(\tanh(\sigma))$ function[15]. The implementation flow chart is shown in Figure 5

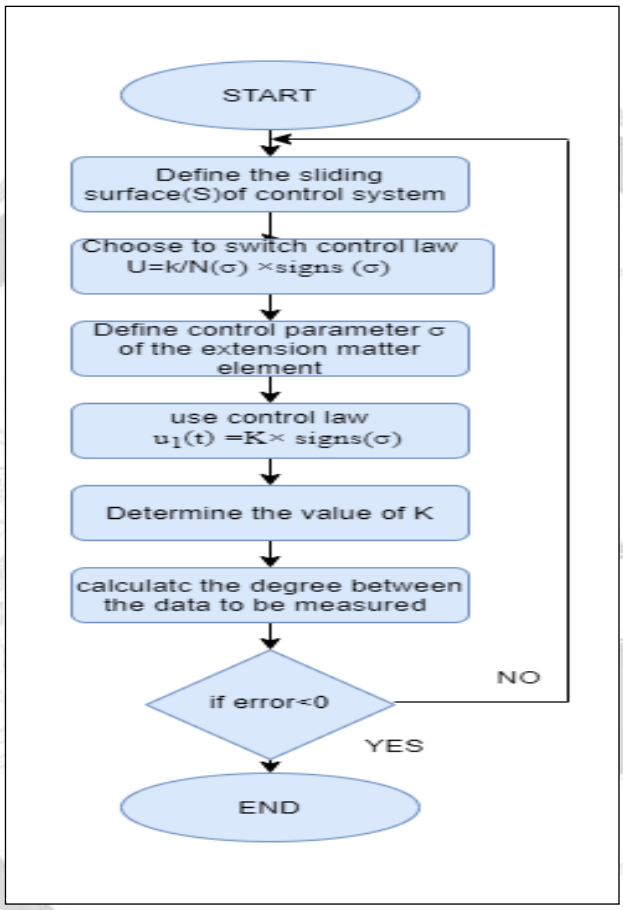

Figure 5: Flow Chart of SMC Implementation

5.Simulation Results

Operation of the SRM motor was simulated using MATLAB Simulink R2020a. The Exponential Sliding mode controller as shown in figure. 6 and, in parallel, a PID controller was also simulated for comparison. The parameters used in the SRM motor of this paper are listed in the Table 1. Various simulations were done according to the cases presented in the following sub-sections to elucidate the speed control and system behavior.

5.1.System Response at the Start

The desired speed reference was 4000RPM. At the beginning, a PID controller was used. Figure. 7 shows a high overshoot and delay time compared to ExpSMC, which will subsequently be used. In the ExpSMC case, the simulation results show a rapid response to reach a steady-state condition with a lower overshoot value. In comparison with Figure (7), the motor speed decreases for a short period of time, then the motor accelerates towards the set point. In the simulation results, the peak speed is 4480 RPM and the desired speed is 4000 RPM, resulting in an overshooting of 12% when using PID control, while the peak speed is 4000 RPM using sliding mode control, where the overshooting is (0.0013) equal to

zero. Table 2 represents both controller responses and Simulation resulted . The gains of the PID controller were set after tuning. They were K_p = 0.3 ,K_i = 1.2and K_d=0

Table 1: SRM Parameters

Parameters	Values
Phase	3
rated power	1.5KW
No_load Speed(RPM)	10000RPM
Rated Speed(RPM)	٤٨٠٠/٦١٠٠RPM
Stator Resistance	0.025Ω
Unaligned inductance (H)	0.314e-3H
Aligned inductance	1.8e-3 H
Rated current	31/35A
No load current	16/17A
Inertia	0.0082J(kg.m2)
Staror/rotor poles	6/4

Table 2: Both Controller Responses

Control	Reference speed Rad/sec	Rise time (ms)	Peak time (ms)	. Overshoot (%)	Settling time (ms)
PID	4000	0.0777	0.1559	12.1779	0.6142
Exponential SMC	4000	0.1885	1.8888	0.0013	0.2660

ISSN: 2616 - 9916
www.journalofbabylon.com | Journal.eng@uobabylon.edu.iq | info@journalofbabylon.com

ISSN: 2616 - 9916
www.journalofbabylon.com | Journal.eng@uobabylon.edu.iq | info@journalofbabylon.com

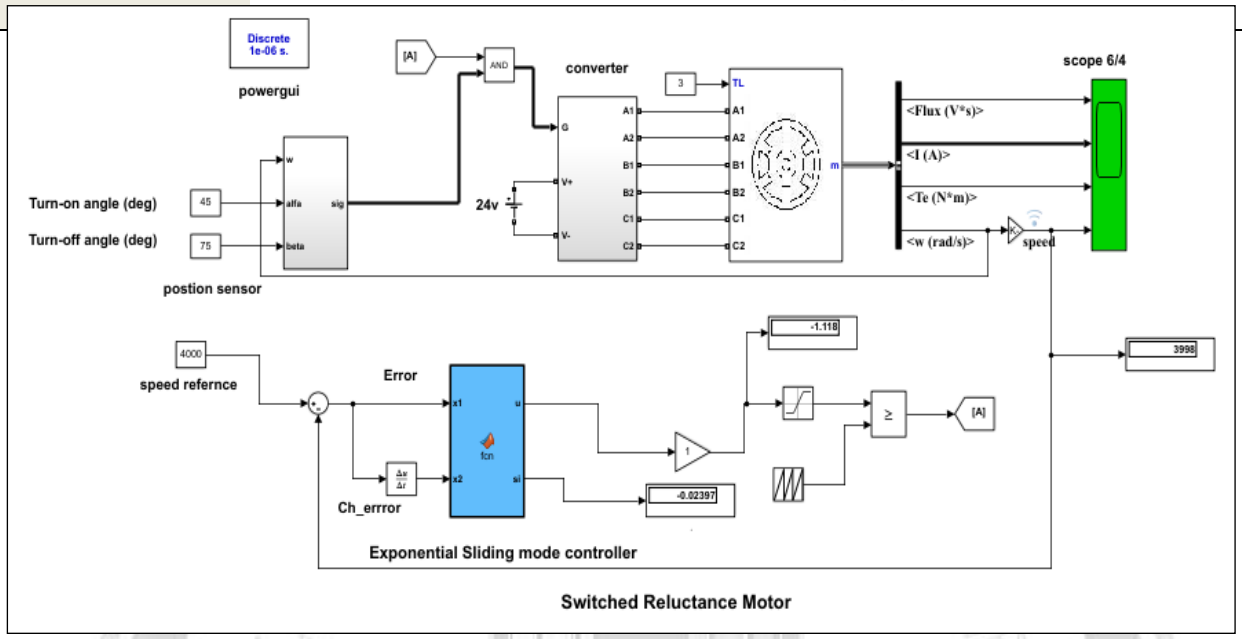

Figure 6: System Simulation by MATLAB Simulink with Exp-SMC

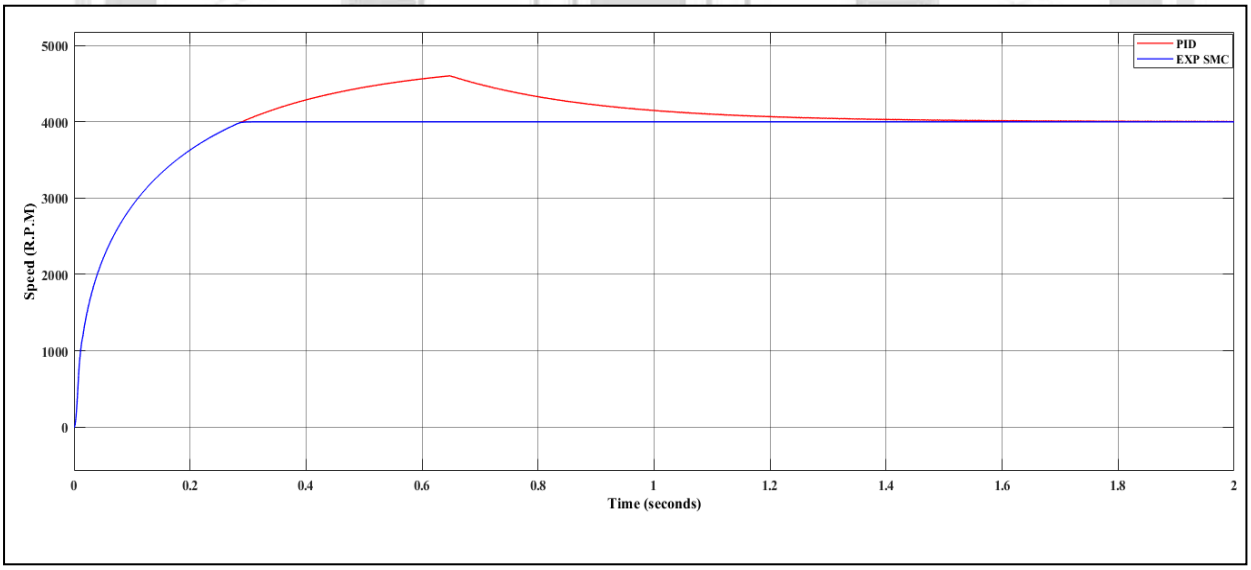

Figure 7: Speed Control Response of SCIM by PID and Exp-SMC

5.2 System Response To Desired Speed Change

In this case, the motor load torque is kept constant at its rated value. The speed of the motor changes from (2000 – 3000) RPM. When a PID controller is used, during speed change, the simulation results show a clear overshoot in the speed response and electrical torque (Te) of the motor, as shown in Figure 8. During this transient period, which lasted for (1 seconds), the Te of the motor reached more than twice its rated value. Also, the speed overshoot is high, but less than shown in Figure 5. This is due to the low-speed differences in the cases examined. Simulation results when Exp-SMC is used are shown in Figure 9. In this case, the transient period lasted with low overshoot in the speed response. Te reaches its rated value very quickly as well. Moreover harmonics due to a chattering phenomenon that is related to Exp-SMC. This chattering leads to a continuous change in the control variable,

ISSN: 2616 - 9916
www.journalofbabylon.com | Journal.eng@uobabylon.edu.iq | info@journalofbabylon.com

which is translated to the driver frequency and modulation index .In this short period, Due to the SRM motor's high starting current and strong starting torque when operating, the motor's Te was high, reaching around five times its rated value . However, this high change might not affect the motor operation.

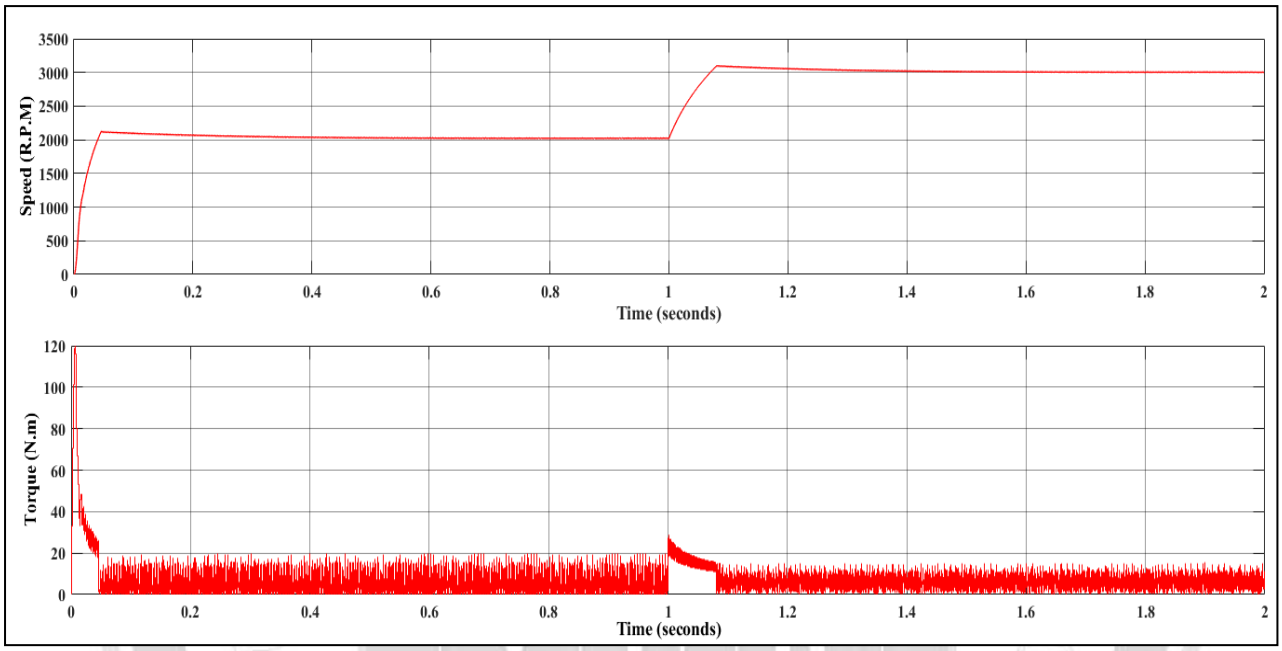

Figure 8: Change in Motor Speed from 2000RPM to 3000 RPM withPID

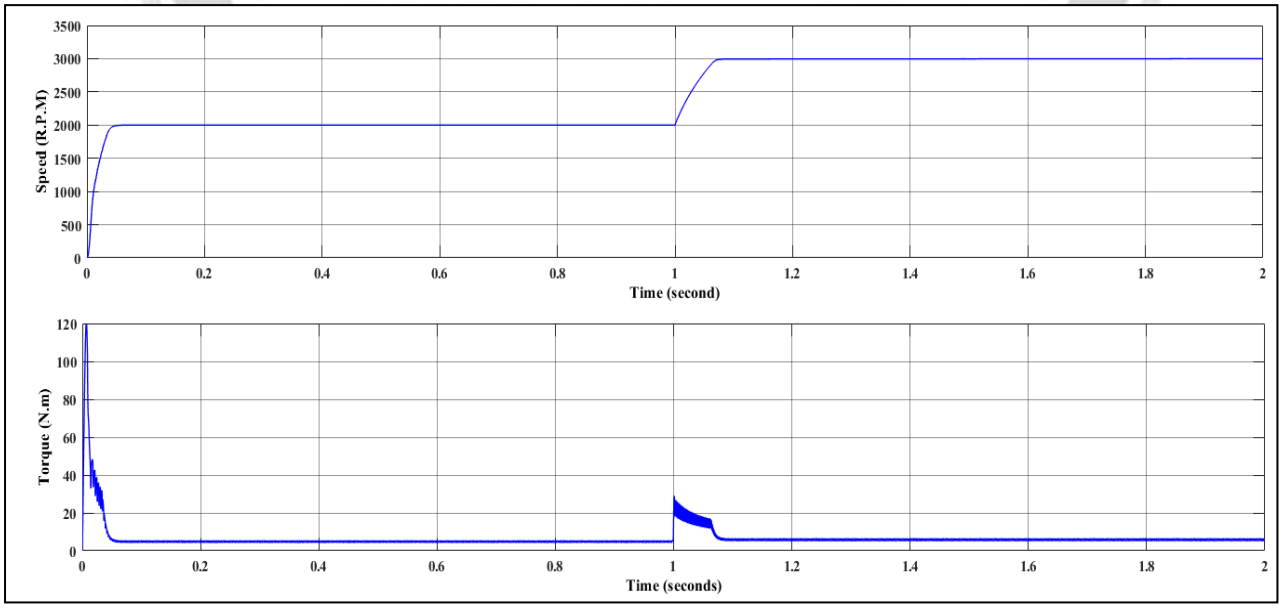

Figure 9: Change in Motor Speed from 2000RPM to 3000 RPM when ExpSMC

5.3. System Response to Load Torques Change

Another case that must be taken into consideration is the load torque change. The load torque was changed from 2N.M to 12N.M, where the full load torque is 12 N.m. When a PID speed controller is used, the stator current of the motor increases in a smooth manner during

the transient period. Also, the speed response exhibits a small dip in its value up to 3000 RPM. The torque of the motor (Te) increases as well, during the transient period. Te shows an overshoots to approximately twice its rated value. The SRM motor current is discontinuous because it operates in a PWM mode that employs a plus sign when one phase is on and a zero sign when the other is off. The transient period of load change lasted for (1 seconds), as shown in Figure 10. In the case of control by ExpSMC, the speed response shows no dip in its value during the transient period as the load is increasedin Figure 11. Te reaches its rated value very quickly as well. Moreover, the stator current changes immediately, but it suffers from harmonics due to a chattering phenomenon that is related to ExpSMC. This chattering leads to a continuous change in the control variable, which is translated to the driver frequency and modulation index. In comparison with a PID controller, EXPSMC in the transient period after load exhibited a change that lasted for (1 seconds). To overcome the issues related to chattering, several techniques can be applied. These include either increasing the switching frequency of the inverter, adding an LC filter between the inverter output terminals and the motor, or use of an unsaturated activation function for the controlling variable. Each of these solutions can be applied singly or in conjunction with others. The factors related to the enhancements are the system nature, size, and cost. Application of all the aforementioned solutions with the experimental work of this paper will be made in a future study.

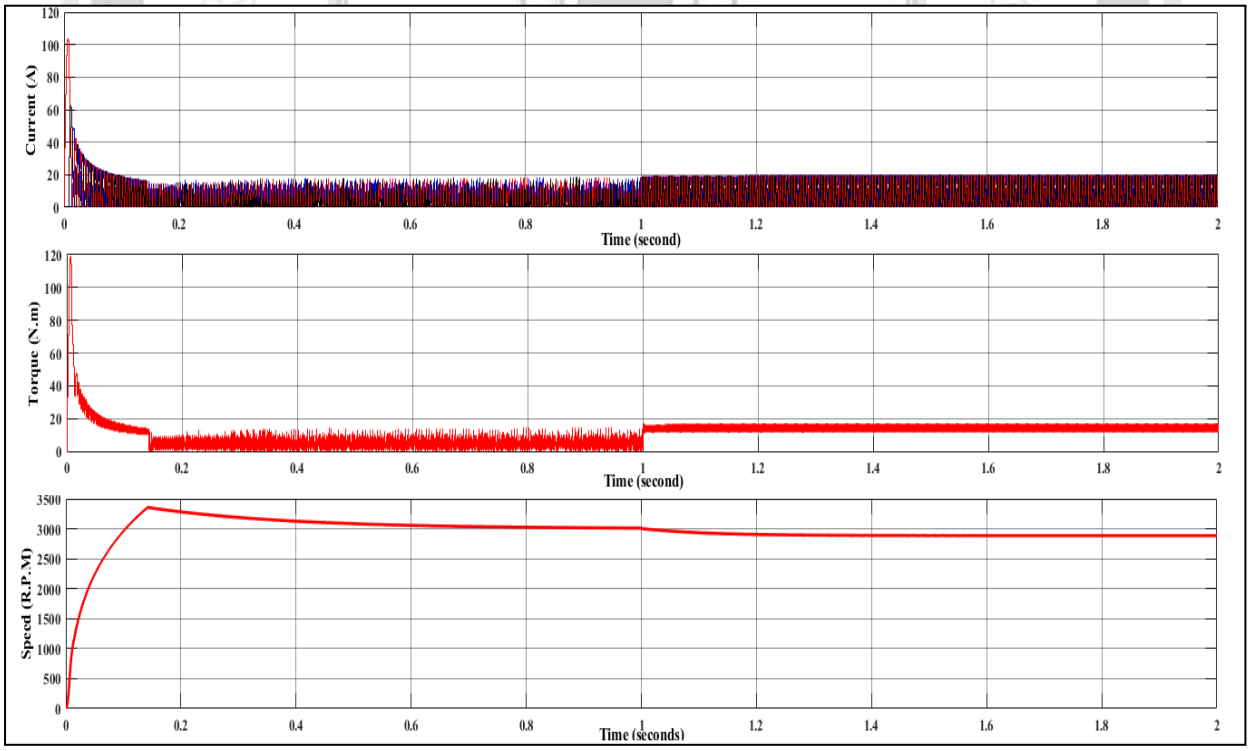

Figure 10: Change in Motor Load Torque from 2 Nm to 12Nm using PID

ISSN: 2616 - 9916
www.journalofbabylon.com | Journal.eng@uobabylon.edu.iq | info@journalofbabylon.com

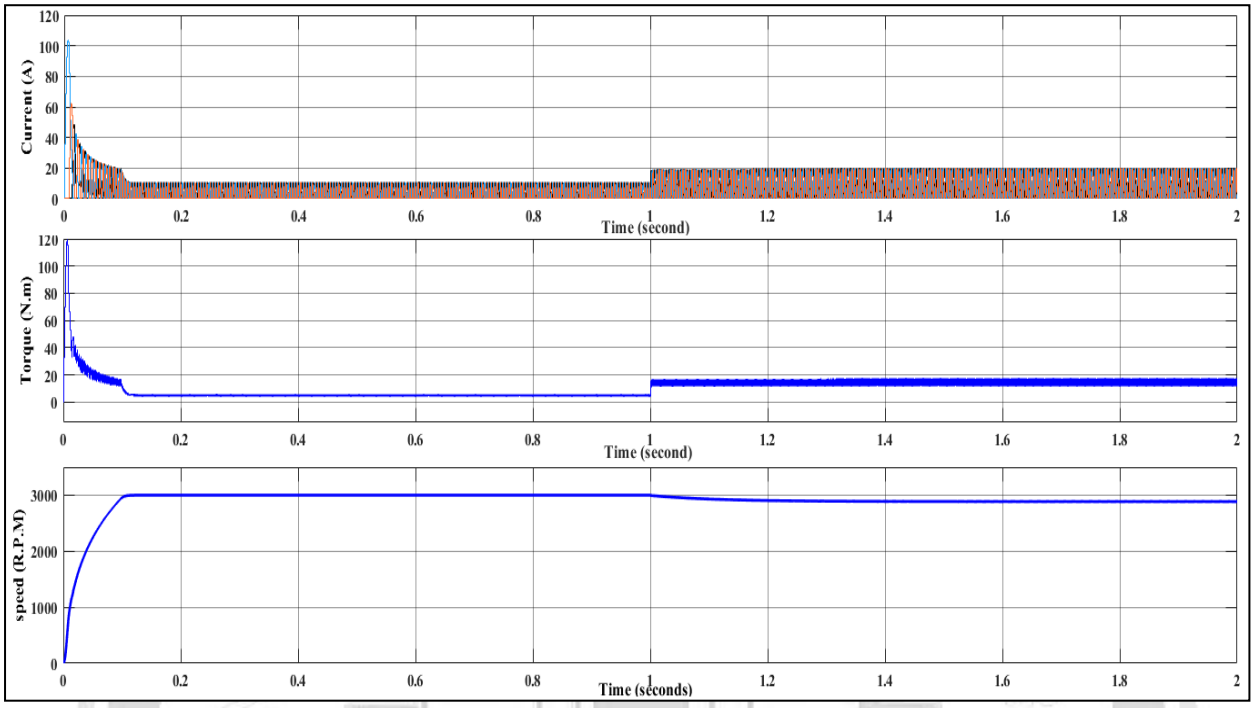

Figure 11: Change in Motor Load Torque from 2 Nm to 12Nm using ExpSMC

Conclusions

This study focused on implementing PID and Exponential SMC controllers for scalar control of the switched reluctance motor. Various simulations were conducted to assess the motor's performance in different operating scenarios. The simulations involved altering the rotational speed with a constant load and varying the load itself, starting from a desired set point. The findings revealed that the Exp-SMC controller exhibited significantly improved characteristics compared to the conventional PID controller, including remarkably low values for overshoot, settling time, and steady-state error. These attributes contribute to its enhanced robustness and faster response. Consequently, the Exp-SMC controller holds potential for effectively regulating the speed of switched reluctance motors in manufacturing processes, industrial applications, and electric vehicles utilizing SRM motors.

ISSN: 2616 - 9916
www.journalofbabylon.com | Journal.eng@uobabylon.edu.iq | info@journalofbabylon.com

ISSN: 2616 - 9916 www.journalofbabylon.com | Journal.eng@uobabylon.edu.iq | info@journalofbabylon.com

References

[1]K. Kiyota, T. Kakishima, and A. Chiba, "Comparison of test result and design stage prediction of switched reluctance motor competitive with 60-kW rare-earth PM motor," *IEEE Transactions on Industrial Electronics,* vol. 61, no. 10, pp. 5712-5721, 2014.

[2]Z. Yang, F. Shang, I. P. Brown, and M. Krishnamurthy, "Comparative study of interior permanent magnet, induction, and switched reluctance motor drives for EV and HEV applications," *IEEE Transactions on Transportation Electrification,* vol. 1, no. 3, pp. 245-254, 2015.

[3]H.-N. Huang, K.-W. Hu, Y.-W. Wu, T.-L. Jong, and C.-M. Liaw, "A current control scheme with back EMF cancellation and tracking error adapted commutation shift for switched-reluctance motor drive," *IEEE Transactions on Industrial Electronics,* vol. 63, no. 12, pp. 7381-7392, 2016.

[4]A. Chiba, K. Kiyota, N. Hoshi, M. Takemoto, and S. Ogasawara, "Development of a rare-earth-free SR motor with high torque density for hybrid vehicles," *IEEE Transactions on Energy Conversion,* vol. 30, no. 1, pp. 175-182, 2014.

[5]E. Öksüztepe, "In-wheel switched reluctance motor design for electric vehicles by using a pareto-based multiobjective differential evolution algorithm," *IEEE Transactions on Vehicular Technology,* vol. 66, no. 6, pp. 4706-4715, 2016.

[6]J. B. Bartolo, M. Degano, J. Espina, and C. Gerada, "Design and initial testing of a high-speed 45-kW switched reluctance drive for aerospace application," *IEEE Transactions on Industrial Electronics,* vol. 64, no. 2, pp. 988-997, 2016.

[7] M. Yildirim *et al.*, "Designing in-wheel switched reluctance motor for electric vehicles," in *2014 16th International Power Electronics and Motion Control Conference and Exposition*, 2014: IEEE, pp. 793-798.

[8]Z. Omaç *et al.*, "Design, analysis, and control of in-wheel switched reluctance motor for electric vehicles," *Electrical Engineering,* vol. 100, pp. 865-876, 2018.

[9]X. Xue, K. W. E. Cheng, T. W. Ng, and N. C. Cheung, "Multi-objective optimization design of in-wheel switched reluctance motors in electric vehicles," *IEEE Transactions on industrial electronics,* vol. 57, no. 9, pp. 2980-2987, 2010.

[10] N. Kurihara, J. Bayless, H. Sugimoto, and A. Chiba, "Noise reduction of switched reluctance motor with high number of poles by novel simplified current waveform at low speed and low torque region," *IEEE Transactions on Industry Applications,* vol. 52, no. 4, pp. 3013-3021, 2016.

[11] X. Liang, G. Li, J. Ojeda, M. Gabsi, and Z. Ren, "Comparative study of classical and mutually coupled switched reluctance motors using multiphysics finite-element modeling," *IEEE Transactions on Industrial Electronics,* vol. 61, no. 9, pp. 5066-5074, 2013.

[12] F. L. Dos Santos, J. Anthonis, F. Naclerio, J. J. Gyselinck, H. Van der Auweraer, and L. C. Góes, "Multiphysics NVH modeling: Simulation of a switched reluctance motor for an electric vehicle," *IEEE Transactions on Industrial Electronics,* vol. 61, no. 1, pp. 469-476, 2013.

[13] Z. Wei, M. Zhao, X. Liu, and M. Lu, "Speed control for SRM drive system based on switching variable proportional desaturation pi regulator," *IEEE Access,* vol. 9, pp. 69735-69746, 2021.

[14] M. Ma, Q. Yang, X. Zhang, F. Li, and Z. Lin, "A switched reluctance motor torque ripple reduction strategy with deadbeat current control," in *2019 14th IEEE Conference on Industrial Electronics and Applications (ICIEA)*, 2019: IEEE, pp. 25-30.

[15] C. Fallaha, M. Saad, and H. Kanaan, "Sliding mode control with exponential reaching law applied on a 3 DOF modular robot arm," in *2007 European Control Conference (ECC)*, 2007: IEEE, pp. 4925-4931.
[16] T. J. E. Miller, *Electronic control of switched reluctance machines*. Elsevier, 2001.
[17] T. J. E. Miller, "Switched reluctance motors and their control," *(No Title)*, 1993.
[18] R. Krishnan, *Switched reluctance motor drives: modeling, simulation, analysis, design, and applications*. CRC press, 2017.
[19] M. S. Islam, I. Husain, R. J. Veillette, and C. Batur, "Design and performance analysis of sliding-mode observers for sensorless operation of switched reluctance motors," *IEEE Transactions on Control systems technology*, vol. 11, no. 3, pp. 383-389, 2003.
[20] K. Ogata, *Modern control engineering*. Prentice hall Upper Saddle River, NJ, 2010.
[21] J.-j. Xue, Y. Wang, H. Li, X.-f. Meng, and J.-y. Xiao, "Advanced fireworks algorithm and its application research in PID parameters tuning," *Mathematical Problems in Engineering*, vol. 2016, 2016.
[22] R. López, "Robust control," ed, 2016.
[23] A. Mehta and B. Naik, *Sliding Mode Controllers for Power Electronic Converters*. Springer, 2019.
[24] R. DeCarlo and S. Zak, "A quick introduction to sliding mode control and its applications," *elettronica, Università degli Studi di Cagliari (Department of Electrical and Electronic Engineering-DIEE, University of Cagliari, Cagliari CA, Italy)*, 2008.
[25] K. Uçak and G. Öke Günel, "An adaptive sliding mode controller based on online support vector regression for nonlinear systems," *Soft Computing*, vol. 24, no. 6, pp. 4623-4643, 2020.
[26] A. G. Iyer, J. Samantaray, S. Ghosh, A. Dey, and S. Chakrabarty, "Sliding Mode Control Using Power Rate Exponential Reaching Law for Urban Platooning," *IFAC-PapersOnLine*, vol. 55, no. 1, pp. 516-521, 2022.

ISSN: 2616 - 9916
www.journalofbabylon.com | Journal.eng@uobabylon.edu.iq | info@journalofbabylon.com

ARTICLE
JOURNAL OF UNIVERSITY OF BABYLON
For ENGINEERING SCIENCES (JUBES)
Vol.31, No.6.| 2023

التحكم الذكي في محرك المعاوقي المفتاحي لتطبيقات المركبات الكهربائية مع طرق التحكم مختلفة

احمد فوزي جاسم فاضل عباس جمعة *علي عبد العباس البكري

قسم هندسة تقنيات القدرة الكهربائية ،الكلية التقنية الهندسية/ المسيب ،جامعة الفرات الاوسط التقنية ،العراق

*كلية المأمون الجامعة

ahmed.fawzi.tcm.22@student.atu.edu.iq

الخلاصة

تستخدم محركات المعاوقي المفتاحي لإنتاج الكثير من عزم الدوران والتي تعمل عند التشبع المغناطيسي العالي. وبالنظر إلى التشبع المغناطيسي العالي، فإن العلاقة بين تيار الطور، وموقع الدوار هي علاقة غير خطية. لذلك فان الضجيج، الاضطرابات، وعزم القصور الذاتي عند التحميل يمكن أن يكون لها جميعا تأثير سلبي على أداء المحرك المعاوقي المفتاحي. في هذه الدراسة تم تطوير وحدة التحكم الانزلاقي. وقد استخدم وحدة التحكم الانزلاقي في تنظيم السرع على مدى واسع بما في ذلك المحرك المعاوقي المفتاحي في السرع العالية والسرع الواطئة وتقارن هذه الدراسة وحدة التحكم الانزلاقي مع وحدة التحكم التناسبي المتكامل التفاضلي في المحرك المعاوقي المفتاحي ذو ٦/٤ اقطاب باستعمال الطرق الامثل للتحكم . ومقارنة سرعة الجزء الدوار مع السرعة المضبوطة .فان وحدة التحكم الانزلاقي المتسارع هو الافضل من حيث الاداء والمتانة في تطبيق السيارات الكهربائية تبعا لنظام السيمولنك المستخدم

الكلمات الدالة: وحدة التحكم الانزلاقي المتسارع، حدة التحكم التناسبي المتكامل التفاضلي، المحرك المعاوقي المفتاحي السيارات الكهربائية.

ISSN: 2616 - 9916
www.journalofbabylon.com | Journal.eng@uobabylon.edu.iq | info@journalofbabylon.com